Author/s:
Ng, AP;Kauppi, M;Metcalf, D;Rago, LD;Hyland, CD;Alexander, WS

Title:
Characterization of thrombopoietin (TPO)-responsive progenitor cells in adult mouse bone marrow with in vivo megakaryocyte and erythroid potential

Date:
2012-02-14

Citation:
Ng, A. P., Kauppi, M., Metcalf, D., Rago, L. D., Hyland, C. D. & Alexander, W. S. (2012). Characterization of thrombopoietin (TPO)-responsive progenitor cells in adult mouse bone marrow with in vivo megakaryocyte and erythroid potential. Proceedings of the National Academy of Sciences of the United States of America, 109 (7), pp.2364-2369. https://doi.org/10.1073/pnas.1121385109.

Publication Status:
In Press

Persistent Link:
https://hdl.handle.net/11343/29079

Characterization of TPO-responsive progenitor cells in adult mouse bone marrow with *in vivo* megakaryocyte and erythroid potential

Ashley P Ng[1,*], Maria Kauppi[1,*], Donald Metcalf[1,2], Ladina Di Rago[1], Craig D Hyland[1], Warren S Alexander[1,2].

[1]The Walter and Eliza Hall Institute of Medical Research, Parkville, Victoria, Australia

[2]Department of Medical Biology, The University of Melbourne, Parkville, Victoria, Australia

*Equal first authors

Running title : Megakaryocyte and erythroid progenitors

BIOLOGICAL SCIENCES: Cell Biology

Key Words : Thrombopoietin, Megakaryocyte, Progenitor

Correspondence**:** Professor Donald Metcalf or Dr Ashley Ng

The Walter and Eliza Hall Institute of Medical Research

1G Royal Parade, Parkville, Victoria, 3052, Australia

Tel: +61-3-9345-2555

Fax: +613-9347-0852

Email: metcalf@wehi.edu.au or ang@wehi.edu.au

Abstract

Hematopoietic progenitor cells are the progeny of hematopoietic stem cells that coordinate production of precise numbers of mature blood cells of diverse functional lineages. Identification of cell surface antigen expression associated with hematopoietic lineage restriction has allowed prospective isolation of progenitor cells with defined hematopoietic potential. To further clarify the cellular origins of megakaryocyte commitment, we have assessed the *in vitro* and *in vivo* megakaryocyte and platelet potential of defined progenitor populations in the adult mouse bone marrow. We show that megakaryocytes arise from $CD150^+$ bipotential progenitors that display both platelet- and erythrocyte-producing potential *in vivo*, and that can develop from the $Flt3^-$ fraction of the pre-granulocyte-macrophage (PreGM) population. We define a bi-potential erythroid-megakaryocyte progenitor population (BEMP), the $CD150^+CD9^{lo}Endoglin^{lo}$ fraction of $Lin^-cKit^+IL7R\alpha^-Fc\gamma RII/III^{lo}Sca1^-$ cells, which contains the bulk of the megakaryocyte colony-forming capacity (CFC) of the bone marrow, including bipotential megakaryocyte-erythroid CFC, and can efficiently generate both erythrocytes and platelets *in vivo*. This fraction is distinct from the $CD150^+CD9^{hi}Endoglin^{lo}$ fraction, which contains bipotential precursors with characteristics of increased megakaryocytic maturation, and the $CD150^+CD9^{lo}Endoglin^{hi}$ fraction, which contains erythroid lineage-committed cells. Finally, we demonstrate that BEMP and $CD150^+CD9^{hi}Endoglin^{lo}$ cells are TPO-responsive and that the latter population specifically expands in the recovery from thrombocytopenia induced by anti-platelet serum.

\body

Introduction

Adult hematopoietic progenitor cells are derived from hematopoietic stem cells (HSCs) in the bone marrow and coordinately produce precise numbers of mature hematopoietic cells of diverse functional lineages. Unlike HSCs, which are rare, hematopoietic progenitors comprise a significant proportion of the adult bone marrow and can undergo significant expansion in times of hematopoietic stress, mediated in large part by hematopoietic cytokines (1). Semi-solid agar culture was the first *in vitro* assay that allowed identification of the myeloid lineage potential of hematopoietic progenitor cells at a clonal level (2). Identification of cell surface antigen expression associated with stem cell activity and lineage restriction allowed prospective isolation of progenitors with defined hematopoietic potential. In the mouse bone marrow, hematopoietic stem cell activity is correlated with expression of cKit and Sca1, and the absence of expression of markers of mature hematopoietic cells of multiple lineages (3) (4). Progenitor cells, defined by *in vitro* colony forming activity, are mainly located within the $Lin^{-}Kit^{+}Sca1^{-}$ fraction (5). This population can be further sub-divided using FcγRII/III and CD34 surface markers (6) to define a common myeloid progenitor (CMP, $CD34^{+}FcγRII/III^{-}$) as well as populations enriched for restricted granulocyte-macrophage potential (GMP, $CD34^{+}FcγRII/III^{+}$) and erythroid and megakaryocyte potential (MEP, $CD34^{-}FcγRII/III^{-}$). The CMP population proved heterogeneous, with Flt-ligand receptor (Flk2/Flt3) and PU.1 expression allowing segregation into granulocyte-monocyte ($Flt3^{+/-}PU.1^{hi}$) or megakaryocyte/erythroid ($Flt3^{-}PU.1^{lo}$) restricted progenitor populations (7).

Defining hematopoietic progenitor cells with megakaryocyte/erythroid potential has

been complicated by the emergence of several immunophenotypic definitions for megakaryocyte and megakaryocyte/erythroid bipotential progenitors. CD41, the integrin IIb subunit, CD150 the founding member of the SLAM family of cell surface receptors, and CD9, a member of the tetraspanin superfamily, have been used in various combinations to define progenitors with megakaryocyte lineage potential within the $Lin^{-}cKit^{+}$ pool (8) (9) (10) (Table S1). However, none of these antigens appear unique to megakaryocyte-restricted cells. For instance, although CD41 expression has been used to define a population of megakaryocyte progenitors (9), ganciclovir treatment of cells expressing thymidine kinase driven by the CD41 promoter leads to suppression of early erythoid-megakaryocytic progenitors *in vivo* and *in vitro* (11).

To further clarify the cellular precursors of committed megakaryocyte cells, we have undertaken a functional assessment of megakaryocyte and platelet potential within the adult mouse bone marrow. We define a $CD150^{+}CD9^{lo}Endoglin^{lo}$ fraction of the $Lin^{-}cKit^{+}IL7R\alpha^{-}Fc\gamma RII/III^{lo}Sca1^{-}$ progenitor population that contains bipotential erythroid-megakaryocyte progenitors (BEMPs). This fraction is distinct from (a) the $CD150^{+}CD9^{hi}Endoglin^{lo}$ fraction, which contains bipotential precursors with characteristics of increased megakaryocytic maturation, and which expands in response to TPO stimulation and anti-platelet serum (APS)-induced thrombocytopenia, and (b) the $CD150^{+}CD9^{lo}Endoglin^{hi}$ fraction, which contains erythroid lineage-committed cells. We also demonstrate that megakaryocyte progenitor cells defined via expression of CD41 retain erythroid potential, and that the $Flt3^{-}$ fraction of the previously defined pre-granulocyte-macrophage (PreGM) population, contains progenitors capable of forming megakaryocytes and erythroid

progenitors in addition to granulocyte/monocyte forming cells (9).

Results

To determine the relative contribution of progenitors in mouse adult bone marrow to megakaryocyte production using semi-solid culture assays, we initially fractionated the $Lin^-cKit^+IL7R\alpha^-Fc\gamma RII/III^{lo}Endoglin^{lo}$ population in mouse adult bone marrow using Sca1 as well as CD150 and CD48, (SI Figure 1, SI Materials and Methods). CD150 has been implicated as a marker of megakaryocyte potential within the hematopoietic progenitor cell pool (8, 9).

Consistent with previous studies (5), the $Sca1^+$ fraction of this population contained almost all the pre-progenitor blast colony-forming cells (CFC), as well as producing colonies containing a diverse range of myeloid cells, including around one-tenth of the megakaryocyte colony-forming potential of the starting population (Table 1, SI Figure 1). The majority of the megakaryocyte colony-forming potential was found within the $Sca1^-$ fraction. Megakaryocyte CFC potential was present within both the $CD150^+Sca1^-$ and $CD150^-Sca1^-$ fractions. The $CD150^+Sca1^-$ fraction contained approximately two-thirds of the megakaryocyte colony-forming potential of the initial population and generated virtually exclusively megakaryocyte containing colonies (Table 1, SI Figure 1). The $CD150^-Sca1^-$ fraction, which includes the previously defined PreGM progenitors (9), generated granulocyte-monocyte colonies as well as megakaryocyte containing colonies (Table 1, Table S1).

The identity of the megakaryocyte colony-forming cells in within the $CD150^+$ progenitor cell population was further investigated by fractionating $Lin^-cKit^+Sca1^-$

IL7Rα$^-$FcγRII/III^{lo}CD150$^+$ cells using CD9 and Endoglin expression into three distinct sub-populations (Figure 1A). Of these, the CD150$^+$CD9^{lo}Endoglin^{hi} population corresponds to the previously defined PreCFU-E population (9) (Table S1, Figure 1C) and demonstrated erythroblast morphology (Figure 1B right panel), and the CD150$^+$CD9^{hi}Endoglin^{lo} cells are immunophenotypically equivalent to previously defined CD9^{hi}MkPs (10) (Table S1, Figure 1C) and showed features of early megakaryocyte differentiation (Figure 1B middle panel). The CD150$^+$CD9^{lo}Endoglin^{lo} fraction was a novel population with an immature morphology without features of erythroid or megakaryocyte differentiation (Figure 1B left panel). This fraction contained all the previously defined PreMegE cells (9) (Table S1, Figure 1C) which comprised 85% of the CD150$^+$CD9^{lo}Endoglin^{lo} population, as well as cells expressing CD41 (SI Figure 2). Each of these populations was tested for colony forming potential *in vitro*. Almost all the megakaryocyte colony-forming potential was within the CD150$^+$CD9^{lo}Endoglin^{lo} fraction (Table 2). A third of the CFCs in this population were definitively bipotential in that they generated colonies containing both megakaryocyte and erythroid cells. In contrast the CD150$^+$CD9^{hi} population had limited clonogenic potential with pure megakaryocyte colonies comprising greater than 90 percent of colonies, in keeping with the more differentiated morphology of these cells. The CD150$^+$Endoglin^{hi} PreCFU-E population had virtually no megakaryocyte colony-forming potential (Table 2). None of these fractions contained significant numbers of granulocyte, macrophage or eosinophil colony-forming cells (Table 2).

In vivo potential of Lin$^-$cKit$^+$IL7Rα$^-$FcγRII/III^{lo}Sca1$^-$CD150$^+$ fractions

To define the *in vivo* potential of progenitors within the Lin$^-$cKit$^+$IL7Rα$^-$

FcγRII/III^{lo}Sca1^{-}CD150^{+} population, we examined the contribution to the peripheral blood of recipient mice injected with GFP-marked sub-fractions (12). The CD9^{hi}Endoglin^{lo} population rapidly generated platelets *in vivo*, with contribution evident within 4 days of transplantation, peak levels at day 7 and a decline thereafter (Figure 2A). The CD9^{lo}Endoglin^{lo} fraction exhibited significant and more sustained platelet-forming capacity. Compared with the CD150^{+}CD9^{hi} population, platelet production by this fraction was delayed, but had not declined at 12 days after transplantation. Each of these populations also displayed robust erythrocyte-forming potential *in vivo* (Figure 2A), but did not generate lymphoid or granulocyte/monocyte cells over this period. On the basis of this activity and clonogenic colony assays, we refer to the Lin^{-}cKit^{+}IL7Rα^{-}FcγRII/III^{lo}Sca1^{-}CD150^{+}CD9^{lo}Endoglin^{lo} fraction as a bipotential erythroid-megakaryocyte precursor population (BEMP). As expected, the Endoglin^{hi}CD9^{lo} PreCFU-E population produced erythrocytes but not platelets (Figure 2A). Intriguingly, and consistent with the capacity to generate megakaryocyte containing colonies *in vitro,* the CD150^{-} component of the Lin^{-}cKit^{+}IL7Rα^{-} FcγRII/III^{lo}Sca1^{-} bone marrow fraction, previously identified as a PreGM fraction (9), demonstrated equivalent, if not superior, platelet-generating capacity compared with the CD150^{+} fractions, in combination with potent erythroid potential (Figure 2A). Consistent with these activities, upon transplantation, GFP-marked PreGM cells generated both GMP and erythroid progenitors within the recipient bone marrow over 4 to 7 days, while granulocyte-macrophage potential was not evident from BEMP cells in the same assay (Figure 2B). Of note, the production of erythroid progenitors from the PreGM fraction was delayed relative to the BEMP cells. This activity was confined to Flt3^{-} progenitor cells within the PreGM fraction: Flt3^{+} PreGM cells yielded granulocyte-monocyte colonies and GMP, but few if any cells with erythroid-

megakaryocyte potential, while Flt3$^-$ PreGM cells generated granulocyte-monocyte colonies and erythroid-megakaryocyte containing colonies *in vitro* and GMP, CFU-E, and CD150$^+$ progenitors *in vivo* (Table S2, SI Figure 4F).

Comparative analysis of progenitors with erythroid-megakaryocyte potential

Flow cytometric analyses were used to determine the relationship of previously defined progenitors with megakaryocyte potential to the BEMP, CD9^{hi}Endoglin^{lo} and CD9^{lo}Endoglin^{hi} fractions of the Lin$^-$cKit$^+$IL7Rα$^-$FcγRII/III^{lo}Sca1$^-$CD150$^+$ bone marrow population. The CD41$^-$ MEP population (8) (Table S1) was contained entirely within the BEMP and CD9^{lo}Endoglin^{hi} fractions (SI Figure 2), while the CD41^{hi}MkP population (9) (Table S1) was distributed between the BEMP and CD9^{hi}Endoglin^{lo} fractions (SI Figure 2). When purified GFP-marked populations were assayed for *in vivo* potential, CD9^{hi}MKPs, CD41^{hi}MKPs, and CD41$^-$MEPs all exhibited robust erythrocyte production in addition to production of platelets (Figure 2A). Lin$^-$ cKit$^+$IL7Rα$^-$FcγRII/III$^-$CD34$^-$Sca1$^-$ MEPs also efficiently generated red blood cells *in vivo*, but were comparatively poor at producing platelets (Figure 2A). It is noteworthy that CD41 expression in these enrichment schemes did not distinguish megakaryocyte-restricted progenitors from their bipotential counterparts. This finding is explained by the observation that CD41^{hi}MkPs overlap with CD150$^+$CD9^{lo}Endoglin^{lo} BEMPs (SI Figure 2). Like BEMPs, CD41$^-$MEPs exhibited sustained production of both erythrocytes and platelets *in vivo* (Figure 2A). In contrast, CD9^{hi} expression, exemplified in both CD9^{hi}MkPs and CD150$^+$CD9^{hi}Endoglin^{lo} fractions, appeared to define a bipotential population with a unique pattern of transient platelet reconstitution (Figure 2A), in keeping with cytomorphological features of more advanced megakaryocyte differentiation (Figure

1B) and limited clonogenicity (Table 2).

Down-regulation of PU.1 expression is associated with restriction of myeloid progenitors to erythroid and megakaryocyte lineage fates (7). Consistent with their *in vivo* potential, PU.1 expression in bipotential BEMP and $CD150^{+}CD9^{hi}Endoglin^{lo}$ progenitors was significantly lower than observed in PreGM or GMP populations, and further down-regulation of PU.1 was evident in erythroid restricted PreCFU-E and CFU-E bone marrow fractions (Figure 2C).

BEMPs are responsive to thrombopoietin-induced megakaryocyte differentiation *in vitro*

In cultures containing a mixture of SCF, IL-3 and EPO, a general stimulus of myeloid, megakaryocytic and erythroid cells, BEMPs generated both $CD9^{hi}Endoglin^{lo}$ and $CD9^{lo}Endoglin^{hi}$ cells during four days in culture, indicative of both megakaryocytes and erythroid cells defined by morphological criteria (Figure 3A,B, SI Materials and Methods). TPO stimulation of BEMPs, in combination with SCF, resulted in an increase in the proportion of $CD9^{hi}Endoglin^{lo}$ cells and megakaryocytes produced, while the combination of EPO and SCF favored accumulation of $CD9^{lo}Endoglin^{hi}$ and recognisable erythroid cells (Figure 3A,B). TPO was a potent stimulus for megakaryocyte differentiation from BEMPs, with TPO+SCF-stimulated megakaryocytes displaying higher DNA ploidy than their EPO+SCF stimulated counterparts (Figure 3C). However, TPO was a relatively poor proliferative stimulus, even in combination with SCF, with the total number of cells generated from BEMPs significantly lower than that generated in response to EPO+SCF or SCF+IL-3+EPO

(Figure 3D). Consistent with the relatively low *in vitro* clonogenic potential and transient *in vivo* platelet-generating capacity of the $CD150^{+}CD9^{hi}Endoglin^{lo}$ fraction, these cells proliferated less than their BEMP counterparts, but were also capable of responding to TPO and EPO with enhanced megakaryocytic and erythroid differentiation respectively (Figure 3D, SI Figure 3). $CD150^{+}CD9^{lo}Endoglin^{hi}$ PreCFU-E cells readily generated erythroid cells in the presence of EPO, but displayed negligible megakaryocyte differentiation in these assays (SI Figure 3).

As expected from the analyses of *in vivo* potential, the PreGM population was capable of granulocyte/monocyte, erythroid and megakaryocyte differentiation and expansion *in vitro*, but unlike BEMPs, did not show a proportional increase in megakaryocyte differentiation in response to TPO+SCF, presumably due to the significant granulocyte formation stimulated by SCF (SI Figure 4A-E).

$CD150^{+}CD9^{hi}Endoglin^{lo}$ cells expand in response to excess TPO or APS-induced thrombocytopenia

We next examined the effect of supra-physiological TPO signaling on the $CD150^{+}$ $Lin^{-}cKit^{+}IL7R\alpha^{-}Fc\gamma RII/III^{lo}Sca1^{-}$ population *in vivo*. While the number of BEMPs was modestly increased in the bone marrow of TPO^{Tg} mice (13), $CD150^{+}CD9^{hi}Endoglin^{lo}$ early megakaryocyte differentiated bi-potential progenitors proportionally doubled at the expense of $CD150^{+}CD9^{lo}Endoglin^{hi}$ Pre-CFU-E cells (Figure 4A). Consistent with these effects reflecting increased TPO signaling, the converse was observed for each of these populations in $Mpl^{-/-}$ mice (14).

We then assessed whether perturbation of $CD150^+$ bipotential progenitor populations toward megakaryocyte differentiation could be induced by acute thrombocytopenia following treatment with anti-platelet serum (APS). APS was administered to wild-type mice, and the numbers of $CD150^+$ bone marrow progenitors, bone marrow megakaryocytes and peripheral blood platelets were analysed during the subsequent days. As previously described, administration of APS resulted in rapid, severe thrombocytopenia, with platelet numbers falling to less than 5% of the pre-treatment level within 2 hours. Recovery was evident 2 days later and platelet numbers returned to normal levels within 4 days of treatment (Figure 4B). Expansion of the $CD150^+CD9^{hi}Endoglin^{lo}$ population was demonstrable on days 1, 2 and day 4 after APS administration, and thereafter returned to levels observed in control mice administered normal saline (Figure 4B). The expansion of these progenitors coincided with the increase in bone marrow megakaryocyte number (Figure 4C) and preceded the recovery in platelet count. The numbers of BEMPs and $CD150^+CD9^{lo}Endoglin^{hi}$ PreCFU-E cells did not alter significantly during the APS recovery period (Figure 4B). The response to APS is likely to be driven to a significant extent by TPO, since rapid recovery of platelet numbers failed to occur in APS-treated *Mpl*$^{-/-}$ mice (Figure 4D).

Discussion

Methods for identification and isolation of myeloid progenitor cell populations according to lineage potential using combinations of surface antigens is a powerful tool in the understanding of physiologic and perturbed hematopoiesis. In this study, we investigated the phenotypic relationships and *in vivo* potential of progenitor cells

with megakaryocyte potential, and summarized our findings in Figure 5. Several cell surface markers have proven useful in defining megakaryocyte potential, including CD150, CD9 and CD41 (Table S1). Here we show that two-thirds of the megakaryocyte colony-forming activity in the adult mouse bone marrow resides in the $CD150^{+}$ fraction of the $Lin^{-}cKit^{+}IL7R\alpha^{-}Fc\gamma RII/III^{lo}Sca1^{-}$ progenitor cell pool, primarily within a $CD9^{lo}Endoglin^{lo}$ population, from which definitive bipotential clones were identified by semi-solid agar colony assays. *In vivo* assays confirmed megakaryocyte lineage potential within this population, which readily generated platelets in transplanted mice. While unable to produce lymphoid or granulocyte/monocyte cells, potent erythroid potential of this population was also evident *in vivo,* leading us to refer to this population as containing bipotential erythroid-megakaryocyte progenitors (BEMP). Unlike prior definitions of bipotential progenitors (Table S1), a proportion of BEMP express CD41. The $CD9^{hi}Endoglin^{lo}$ component of the $CD150^{+}$ progenitor fraction retained bipotential platelet-erythroid potential *in vivo*, but unlike BEMPs, included cells with morphological characteristics of increased megakaryocyte differentiation. Indeed, *in vivo*, the $CD9^{hi}Endoglin^{lo}$ population generated platelets more quickly and more transiently than BEMPs. These observations, combined with the reduced megakaryocyte colony-forming activity of the $CD9^{hi}Endoglin^{lo}$ population relative to BEMPs, implies that the former population contains more mature, less proliferative megakaryocyte/platelet progenitors. The $CD9^{lo}Endoglin^{hi}$ portion of the $CD150^{+}$ progenitor fraction has previously been described as a PreCFU-E population (9) and, as anticipated, lacked megakaryocyte colony forming capacity and *in vivo* platelet potential, but efficiently produced red blood cells. These observations are consistent with a process of maturation in which the $CD9^{lo}Endoglin^{lo}$ BEMPs are the precursors of $CD9^{hi}Endoglin^{lo}$ and

$CD9^{lo}Endoglin^{hi}$ daughter populations, the up-regulation of CD9 being a marker of retained megakaryocyte potential and acquisition of high Endoglin expression correlating with erythroid restriction.

An unexpected outcome of the *in vivo* comparison of distinct bone marrow fractions with megakaryocyte progenitor activity was the observation that all such populations displayed significant erythroid lineage potential in addition to platelet-generating capacity. MkPs defined via expression of CD9 ($CD9^{hi}$MkP, Table S1), or CD41 ($CD41^{hi}$ MkP, Table S1) both readily generated red blood cells when transplanted into recipient mice. Indeed, none of the populations examined displayed purely megakaryocyte/platelet restriction *in vivo*. The final stages of megakaryocyte differentiation may therefore involve production of immature megakaryocytes, or low proliferative potential precursors, directly from bipotential progenitor cells.

It is also noteworthy that the PreGM population, defined as the $CD150^{-}Endoglin^{-}$ fraction of the $Lin^{-}cKit^{+}IL7R\alpha^{-}Fc\gamma RII/III^{lo}Sca1^{-}$ progenitor cell pool, exhibited megakaryocyte colony-forming capacity *in vitro* and the capacity to produce platelets and erythrocytes *in vivo*. Previous studies with this PreGM fraction identified modest production of megakaryocytes and erythroid cells *in vitro* and platelet potential *in vivo* (9). Our results showed not only that the PreGM population has *in vivo* erythroid potential, but that on a per-cell basis, erythroid-megakaryocyte activity appeared as potent as that displayed by the restricted bipotential erythroid-megakaryocyte progenitor populations under study. This activity was restricted to $Flt3^{-}$ PreGM cells. As GMP, CFU-E and $CD150^{+}$ cells could develop from these cells *in vivo*, this

suggests that common myeloid progenitor cells may potentially reside within this fraction.

Among the fractions of $Lin^{-}cKit^{+}IL7R\alpha^{-}Fc\gamma RII/III^{lo}Sca1^{-}CD150^{+}$ compartment defined by levels of CD9 and Endoglin expression, *in vivo* expansion of the $CD9^{hi}Endoglin^{lo}$ population was most prominent in response to elevated TPO concentration in transgenic mice and was selectively reduced in mice lacking the TPO receptor, c-Mpl. As the proliferative capacity of the $CD9^{hi}Endoglin^{lo}$ fraction in cultures containing TPO was relatively low, it seems likely that the TPO-driven expansion of $CD9^{hi}Endoglin^{lo}$ cells is driven in significant part from maturation of precursors such as the BEMP. The observation that the $CD9^{hi}Endoglin^{lo}$ fraction is similarly selectively expanded during recovery from APS-induced thrombocytopenia, a process dependent on intact TPO signaling, suggests that these cells make an important contribution to TPO-driven megakaryocyte and platelet production, not only in steady-state hematopoiesis, but in also in times of acute need.

Materials and Methods

Mice. C57BL/6 mice were analyzed at 7-10 weeks of age. Mice expressing the *Aequorea victoria* green fluorescent protein (GFP) protein under the human ubiquitin C promoter were obtained from Jackson Laboratories (Maine, USA) (12). $PU.1^{gfp}$ reporter strain (7) and mice carrying the TPO^{Tg} (13) and $Mpl^{-/-}$ (14) alleles were derived as previously described. See SI Materials and Methods for details of transplantation. Experimental thrombocytopenia was generated via tail vein injection of rabbit anti-mouse platelet serum (APS, Cedarlane). Experiments were performed

using procedures approved by The Walter and Eliza Hall Institute of Medical Research Animal Ethics Committee.

Hematology and histology. Blood was collected into tubes containing EDTA (Sarstedt) and platelet counts obtained with an Advia 120 analyzer (Bayer). Analysis of erythrocytes and platelets was performed after blood was suspended in buffered saline glucose citrate buffer and single cell suspensions from bone marrow were prepared in balanced salt solution (See SI Materials and Methods). Clonal analysis of bone marrow cells in semi-solid agar cultures and liquid cultures of progenitor cells are described in SI Materials and Methods. Flow cytometry analysis was performed using an LSRII (Becton Dickinson) or cells sorted using a FACS Aria II (Becton Dickinson) flow cytometers after antibody staining ± lineage depletion (See SI Materials and Methods). Cytocentrifuge preparations were stained with May-Grunwald-Giemsa prior to microscopic examination. Images were acquired using a Nikon Eclipse E600 microscope, 4x/1.3 NA or 100x/1.3 NA Oil objective with AxioCam Hrc and AxioVision 3.1 image acquisition software. Femurs were fixed in 10% buffered formalin, embedded in paraffin, and 1 to 3μm sections were stained with hematoxylin and eosin for megakaryocyte enumeration via light microscopy.

Acknowledgements

We thank Stephen Nutt and Sebastian Carotta for their generous gift of *PU.1*^{gfp} mice, Lauren Wilkins, Merle Dayton, Kelly Trueman, and Jaclyn Gilbert for excellent animal husbandry, Jason Corbin and Janelle Lochland for excellent technical assistance. This work was supported by a Program Grant (461219), Fellowships (W.S.A., A.P.N.) and Independent Research Institutes Infrastructure Support Scheme Grant (361646) from the Australian National Health and Medical Research Council, the Carden Fellowship Fund (D.M.) of the Cancer Council, Victoria, a HSANZ/AMGEN New Investigator Scholarship (A.P.N.), Cure Cancer Australia /Leukaemia Foundation Postdoctoral Fellowship (A.P.N.), the Australian Cancer Research Fund, and a Victorian State Government Operational Infrastructure Support grant.

References

1. Metcalf D (2010) The colony-stimulating factors and cancer. *Nat Rev Cancer* 10(6):425-434.
2. Bradley TR & Metcalf D (1966) The growth of mouse bone marrow cells in vitro. *Aust J Exp Biol Med Sci* 44(3):287-299.
3. Spangrude GJ, Heimfeld S, & Weissman IL (1988) Purification and characterization of mouse hematopoietic stem cells. *Science* 241(4861):58-62.
4. Okada S*, et al.* (1992) In vivo and in vitro stem cell function of c-kit- and Sca-1-positive murine hematopoietic cells. *Blood* 80(12):3044-3050.
5. Metcalf D*, et al.* (2009) Murine hematopoietic blast colony-forming cells and their progeny have distinctive membrane marker profiles. *Proc Natl Acad Sci U S A* 106(45):19102-19107.
6. Akashi K, Traver D, Miyamoto T, & Weissman IL (2000) A clonogenic common myeloid progenitor that gives rise to all myeloid lineages. *Nature* 404(6774):193-197.
7. Nutt SL, Metcalf D, D'Amico A, Polli M, & Wu L (2005) Dynamic regulation of PU.1 expression in multipotent hematopoietic progenitors. *J Exp Med* 201(2):221-231.
8. Rieger MA, Smejkal BM, & Schroeder T (2009) Improved prospective identification of megakaryocyte-erythrocyte progenitor cells. *Br J Haematol* 144(3):448-451.
9. Pronk CJ*, et al.* (2007) Elucidation of the phenotypic, functional, and molecular topography of a myeloerythroid progenitor cell hierarchy. *Cell Stem Cell* 1(4):428-442.
10. Nakorn TN, Miyamoto T, & Weissman IL (2003) Characterization of mouse clonogenic megakaryocyte progenitors. *Proc Natl Acad Sci U S A* 100(1):205-210.
11. Tronik-Le Roux D, Roullot V, Schweitzer A, Berthier R, & Marguerie G (1995) Suppression of erythro-megakaryocytopoiesis and the induction of reversible thrombocytopenia in mice transgenic for the thymidine kinase gene targeted by the platelet glycoprotein alpha IIb promoter. *J Exp Med* 181(6):2141-2151.
12. Schaefer BC, Schaefer ML, Kappler JW, Marrack P, & Kedl RM (2001) Observation of antigen-dependent CD8+ T-cell/ dendritic cell interactions in vivo. *Cell Immunol* 214(2):110-122.
13. de Graaf CA*, et al.* (2010) Regulation of hematopoietic stem cells by their mature progeny. *Proc Natl Acad Sci U S A* 107(50):21689-21694.
14. Alexander WS, Roberts AW, Nicola NA, Li R, & Metcalf D (1996) Deficiencies in progenitor cells of multiple hematopoietic lineages and defective megakaryocytopoiesis in mice lacking the thrombopoietic receptor c-Mpl. *Blood* 87(6):2162-2170.

Figure legends

Figure 1. Fractionation of Lin$^-$cKit$^+$Sca1$^-$IL7Rα$^-$FcγRII/III^{lo}CD150$^+$ bone marrow with CD9 and Endoglin. (A) Flow cytometry fractionation of Lin$^-$cKit$^+$Sca1$^-$IL7Rα$^-$FcγRII/III^{lo}CD150$^+$ bone marrow cells by Endoglin and CD9 expression into CD9^{lo}Endoglin^{lo} , CD9^{hi}Endoglin^{lo}, and CD9^{lo}Endoglin^{hi} populations. Isotype control (contour plot). (B) CD9^{lo}Endoglin^{lo} (left panel), CD9^{hi}Endoglin^{lo} (middle panel) and CD9^{lo}Endoglin^{hi} (right panel) cytocentrifuge preparations stained with May-Grunwald-Giemsa. (C) Comparison of CD9^{lo}Endoglin^{lo}, CD9^{hi}Endoglin^{lo} and CD9^{lo}Endoglin^{hi} Lin$^-$cKit$^+$Sca1$^-$IL7Rα$^-$FcγRII/III^{lo}CD150$^+$ bone marrow fractions with CD9^{hi}MkP, Pre-CFU-E and PreMegE populations (Table S1) by flow cytometry.

Figure 2. *In vivo* potential of transplanted progenitor cells. Transplantation of 1000 GFP-marked cells (12) from purified cell populations into sublethally irradiated recipients (SI Materials and Methods). (A) Percentage contribution to erythrocytes and platelets in peripheral blood from GFP-marked donor-derived cells on days 4, 7 and 12 after transplantation. Means ± standard deviations (S.D.) from 2-3 independent donors each into 3-4 recipients. Y axis $\log_2$ scale. (B) Analysis of Lin$^-$cKit$^+$ bone marrow 4 and 7 days after transplantation with GFP-marked donor PreGM or BEMP cells. Formation of GMP, CMP and MEP (upper panels) and PreCFU-E, CFU-E (lower panels) progenitor populations. Donor cells (Red). Recipient cells (Gray). Representative analysis from three independent donors is shown. (C) Expression of *PU.1*^{gfp} (7) in arbitrary mean fluorescence intensity (MFI) units for each progenitor cell population indicated (Table S1, Table 2). (Left) MFI means ± S.D. from 4 mice for each population. (Right) Representative MFI profiles. $P < 0.0001$ by repeated

measures ANOVA of all progenitor populations. Tukey's multiple comparison of means; $P < 0.05$ for comparison between all populations except between BEMPs and $CD150^{+}CD9^{hi}Endoglin^{lo}$ cells (NS = not significant).

Figure 3. *In vitro* responses of $Lin^{-}cKit^{+}Sca1^{-}IL7R\alpha^{-}Fc\gamma RII/III^{lo}CD150^{+}$ progenitor cells to cytokine stimulation. Liquid culture of sorted progenitor cells after 4 days with cytokine combinations indicated (SCF, 20ng/mL; IL-3, 10ng/mL; EPO, 2IU/mL; TPO, 200ng/mL). (A) May-Grunwald-Giemsa-stained cytocentrifuge preparations (x1000 magnification) of differentiated cells derived from BEMPs. M, megakaryocyte; E, erythroid. (B) Flow cytometry analysis. $CD150^{+}CD9^{hi}$ megakaryocytes (blue), $CD150^{-}CD9^{lo}Endoglin^{hi}$ erythroid progenitors (red). $*P_{adj}<0.05$ when compared to SCF, IL3 and EPO, $**P_{adj} < 0.05$ when compared to SCF and EPO. (C) DNA ploidy of $CD150^{+}CD9^{hi}Endoglin^{lo}$ megakaryocytes generated from BEMP. $*P_{adj}<0.05$ when compared to SCF, IL3 and EPO, $**P_{adj}<$ 0.05 when compared to SCF and EPO (D) Proliferation of purified BEMP, $CD9^{hi}Endoglin^{lo}$ and $CD9^{lo}Endoglin^{hi}$ cells. $*P_{adj}<0.026$ comparing $CD9^{hi}Endoglin^{lo}$ to $CD9^{lo}Endoglin^{hi}$ progenitors. $**P_{adj} < 0.007$ comparing $CD9^{hi}Endoglin^{lo}$ to BEMP cells, $***P_{adj} < 0.007$ comparing SCF+TPO with SCF+IL3+EPO. Statistical analysis by unpaired t-test of 3 biological replicates with Holm modification of Bonferroni correction for multiple testing.

Figure 4. Responses of $Lin^{-}cKit^{+}Sca1^{-}IL7R\alpha^{-}Fc\gamma RII/III^{lo}CD150^{+}$ progenitor cells to excess TPO and APS treatment *in vivo*. (A) BEMP, $CD9^{hi}Endoglin^{lo}$ and $CD9^{lo}Endoglin^{hi}$ populations in wild-type, TPO^{Tg} (13) and $Mpl^{-/-}$ (14) mice. Relative

proportions shown as means ± S.D. from 6 mice per genotype. *P_{adj} < 0.04 for comparison with wild-type by unpaired t-test, with Holm modification of Bonferroni correction for multiple testing. (B-D) Analysis of mice treated with APS. (B) (Upper panel) Megakaryocytes per high powered field (hpf) across sternum and femur sections. (Middle panel) Peripheral blood platelet count. (Lower panel) Ratio of BEMP, $CD9^{hi}Endoglin^{lo}$ and $CD9^{lo}Endoglin^{hi}$ cells after APS treatment compared to normal saline treated controls. Mean ± S.D. from 6 mice per time point. *P <0.02 by unpaired t-test, demonstrating an absolute increase in $CD9^{hi}Endoglin^{lo}$ cells at 2 hours, day 1, day 2 and day 4 after APS, and a decrease in $CD9^{lo}Endoglin^{hi}$ progenitors at day 2 after APS. (C) The number of $CD150^{+}CD9^{hi}Endoglin^{lo}$ cells per viable bone marrow cells compared to the number of megakaryocytes per hpf following APS, with Pearson correlation co-efficient (r) and P value shown. (D) Response of *Mpl*$^{-/-}$ and wild-type mice following APS. The relative number of platelets after APS treatment relative to normal saline treated genotype matched mice. Mean ± S.D. from 3-6 mice per genotype per treatment. * P < 0.002 by student's two-tailed t-test.

Figure 5. Origin of erythroid and megakaryocyte progenitors. Lineage restriction, suggested hierarchical relationships, and response of myeloid progenitor cell populations examined to thrombopoietin (TPO) or anti-platelet serum (APS). Refer to Table S1 for details of immunophenotypes of PreGM (white, green), GMP (green), PreCFU-E (red) and CFU-E (red), and Figure 1A for definitions of $CD9^{lo}Endoglin^{lo}$ BEMP (light purple) and $CD9^{hi}Endoglin^{lo}$ (blue) progenitor populations.

Table Legends

Table 1. Colony-forming potential of fractions of $Lin^{-}cKit^{+}IL7R\alpha$ $Fc\gamma RII/III^{lo}Endoglin^{lo}$ adult bone marrow

Mean colony counts ± standard deviation (S.D.) per 100 cells from 4 replicate experiments using a combined stimulus of SCF (100ng/mL), IL-3 (10ng/mL) and EPO (4IU/mL). G, granulocyte; GM, granulocyte-macrophage; M, macrophage; Eo, eosinophil; Meg, megakaryocyte colonies, including colonies of megakaryocytes and erythroid cells. % $cKit^{+}$ fraction; percentage contribution of each fraction to $Lin^{-}cKit^{+}$ $IL7R\alpha^{-}Fc\gamma RII/III^{lo}Endoglin^{lo}$ bone marrow with means ± S.D. from 4 mice (SI Figure 1). Meg contribution; percentage contribution to megakaryocyte CFC of each fraction, calculated by adjusting contribution to % $cKit^{+}$ fraction by relative ability of cells to form megakaryocyte colonies.

Table 2. Colony-forming potential of fractions of $Lin^{-}cKit^{+}Sca1^{-}IL7R\alpha^{-}$ $Fc\gamma RII/III^{lo}CD150^{+}$ adult bone marrow

Mean colony counts ± S.D. per 100 cells from four replicate experiments using a combined stimulus of SCF, IL-3 and EPO. G, granulocyte; GM, granulocyte-macrophage; M, macrophage; Eo, eosinophil; Meg, megakaryocyte colonies, including colonies of megakaryocytes and erythroid cells. % of $CD150^{+}$ fraction; percentage contribution each population to $Lin^{-}cKit^{+}Sca1^{-}IL7R\alpha^{-}Fc\gamma RII/III^{lo}CD150^{+}$ adult bone marrow with means ± S.D. from 6 mice. Meg contribution; percentage contribution to megakaryocyte CFC of each fraction, calculated by adjusting contribution to % of $CD150^{+}$ fraction by relative ability of cells to form megakaryocyte colonies.

Figure 1

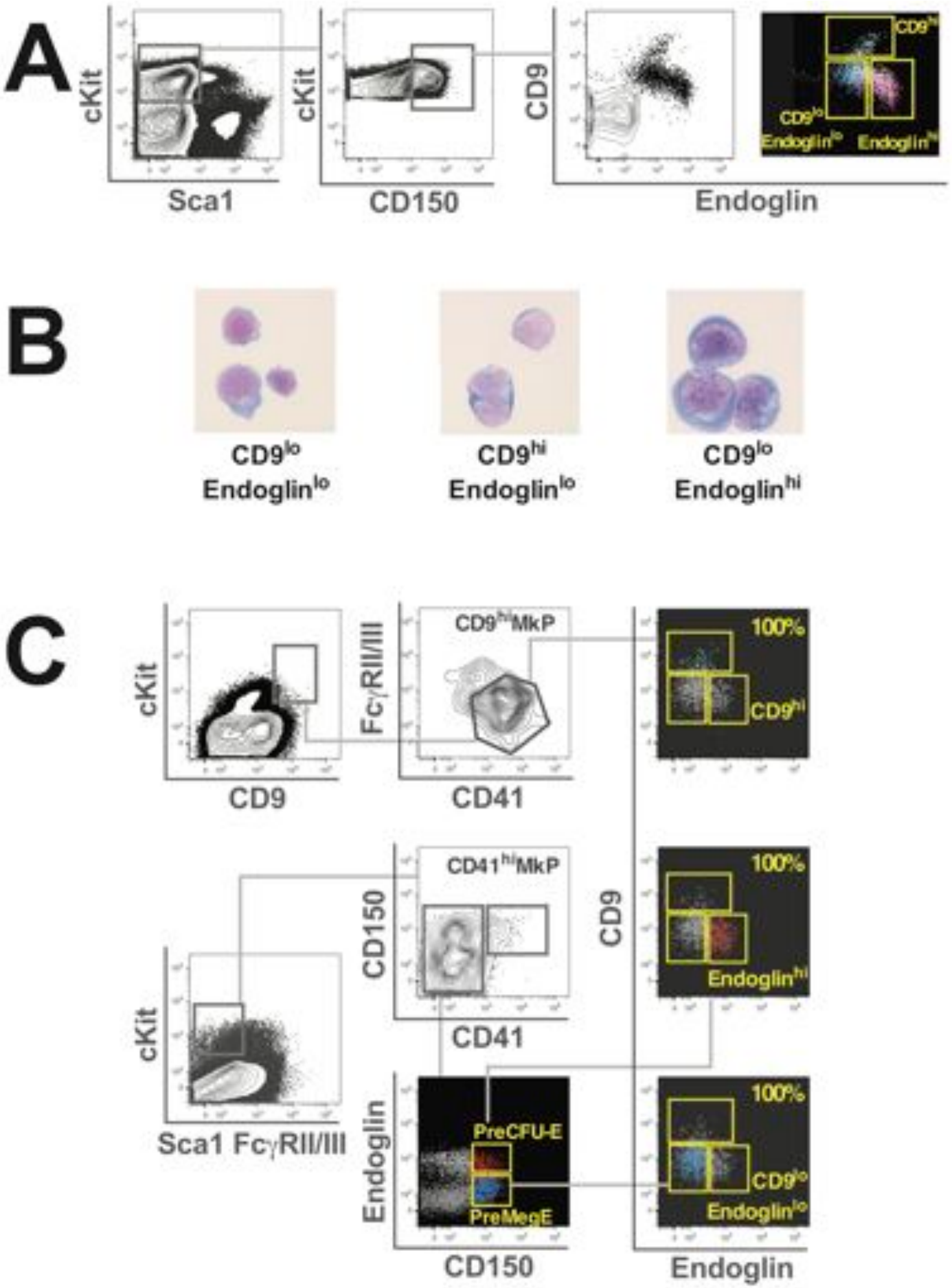
A
cKit
Sca1
cKit
CD150
CD9
Endoglin
CD9hi
CD9lo Endoglinlo
Endoglinhi
B
CD9lo Endoglinlo
CD9hi Endoglinlo
CD9lo Endoglinhi
C
cKit
CD9
FcγRII/III
CD9hiMkP
CD41
100%
CD9hi
cKit
Sca1 FcγRII/III
CD150
CD41hiMkP
CD41
CD9
100%
Endoglinhi
Endoglin
PreCFU-E
PreMegE
CD150
100%
CD9lo
Endoglinlo
Endoglin

Figure 2

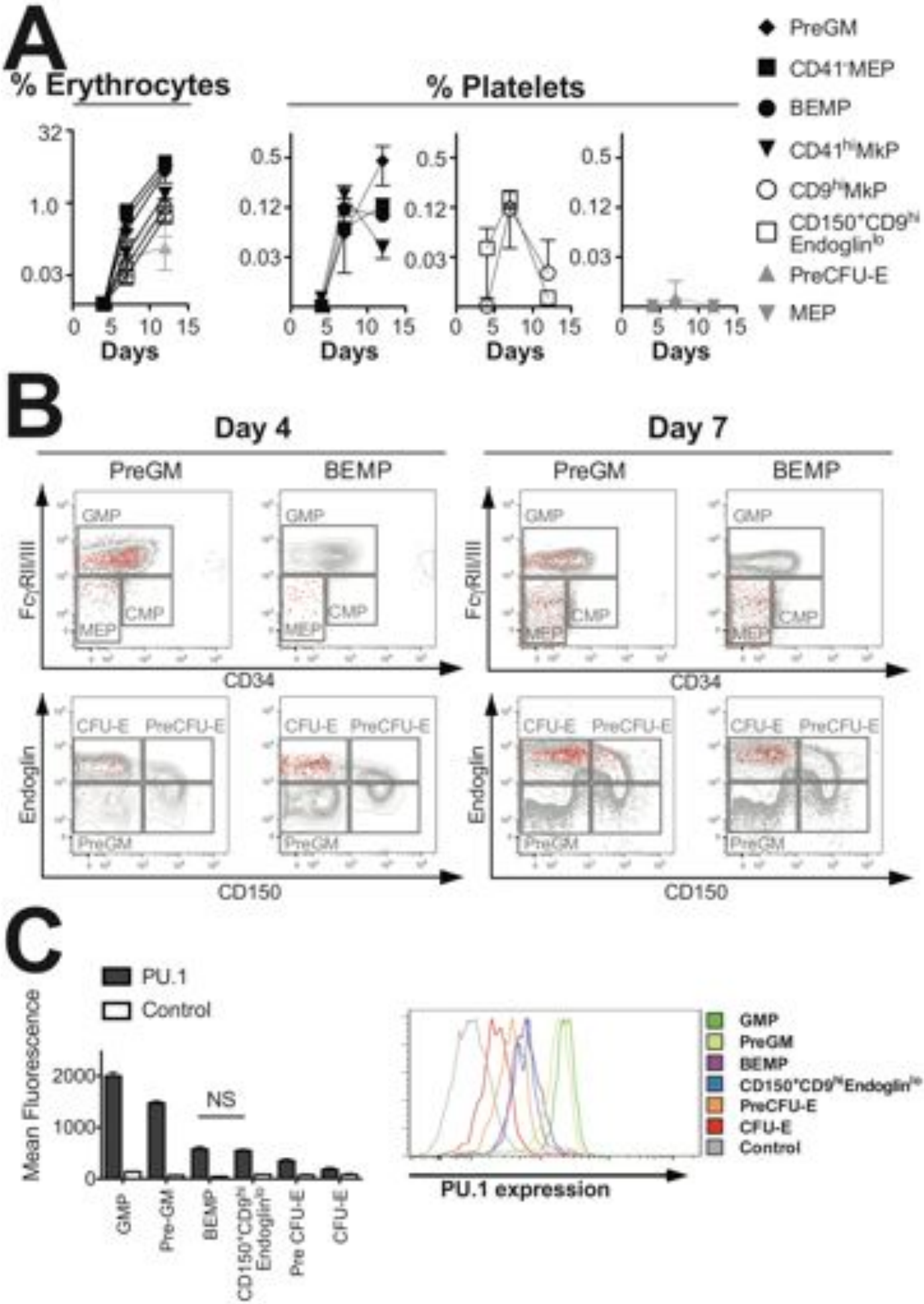
A
% Erythrocytes
% Platelets
PreGM
CD41+MEP
BEMP
CD41hiMkP
CD9hiMkP
CD150+CD9hi Endoglinlo
PreCFU-E
MEP
Days
B
Day 4
Day 7
PreGM
BEMP
GMP
CMP
MEP
FcγRII/III
CD34
CFU-E
PreCFU-E
Endoglin
CD150
C
PU.1
Control
Mean Fluorescence
NS
GMP
Pre-GM
BEMP
CD150+CD9hi Endoglinlo
Pre CFU-E
CFU-E
PU.1 expression
GMP
PreGM
BEMP
CD150+CD9hiEndoglinlo
PreCFU-E
CFU-E
Control

Figure 3

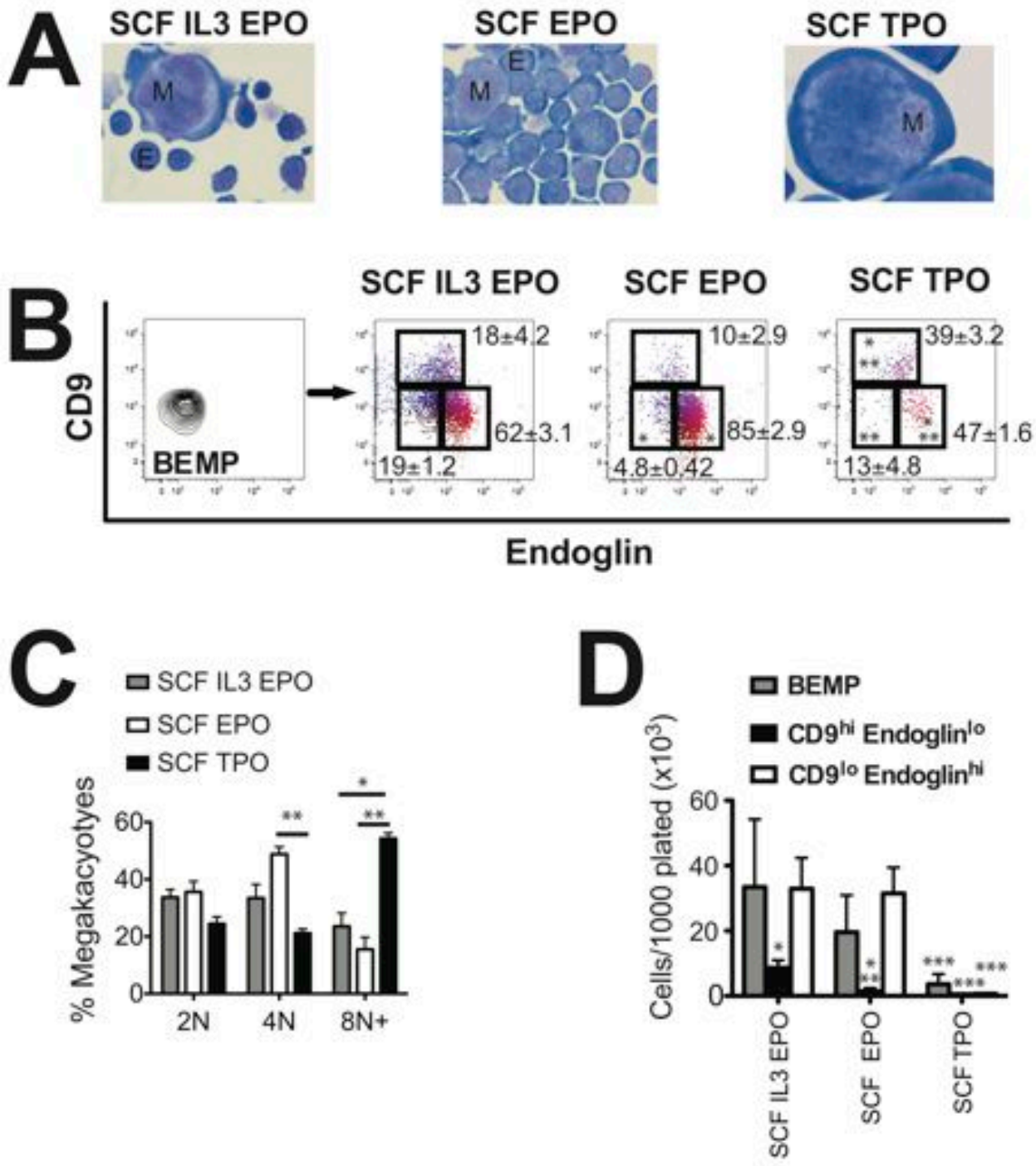
A
SCF IL3 EPO
SCF EPO
SCF TPO
M
E
B
SCF IL3 EPO
SCF EPO
SCF TPO
CD9
Endoglin
BEMP
18±4.2
62±3.1
19±1.2
10±2.9
85±2.9
4.8±0.42
39±3.2
47±1.6
13±4.8
C
SCF IL3 EPO
SCF EPO
SCF TPO
% Megakacyotyes
2N
4N
8N+
D
BEMP
CD9hi Endoglinlo
CD9lo Endoglinhi
Cells/1000 plated (x10³)
SCF IL3 EPO
SCF EPO
SCF TPO

Figure 4

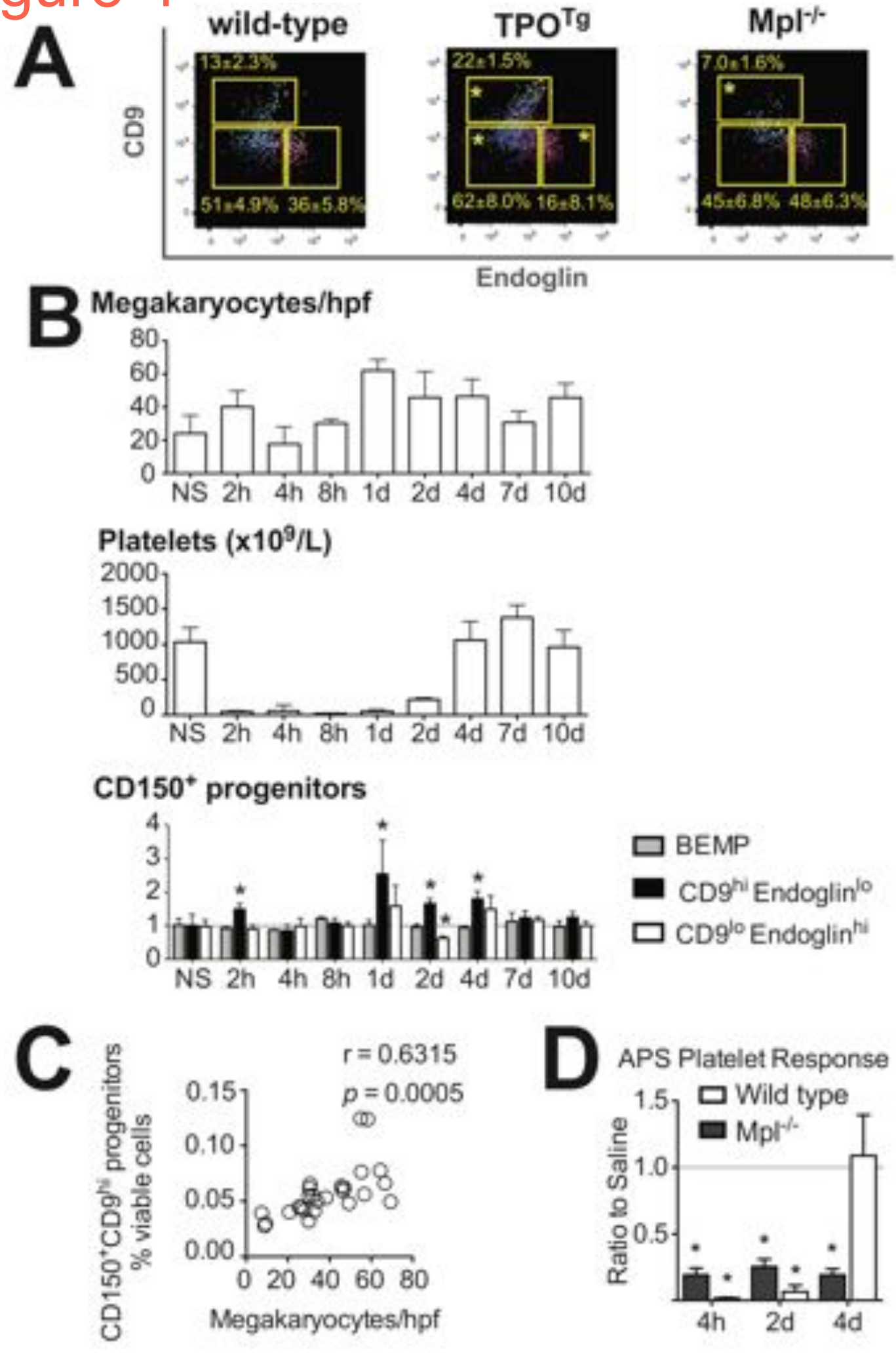
A
wild-type
TPO^Tg
Mpl^-/-
CD9
Endoglin
13±2.3%
51±4.9%
36±5.8%
22±1.5%
62±8.0%
16±8.1%
7.0±1.6%
45±6.8%
48±6.3%
B
Megakaryocytes/hpf
Platelets (x10^9/L)
CD150+ progenitors
NS
2h
4h
8h
1d
2d
4d
7d
10d
BEMP
CD9^hi Endoglin^lo
CD9^lo Endoglin^hi
C
r = 0.6315
p = 0.0005
CD150+CD9hi progenitors % viable cells
Megakaryocytes/hpf
D
APS Platelet Response
Wild type
Mpl^-/-
Ratio to Saline
4h
2d
4d

Figure 5

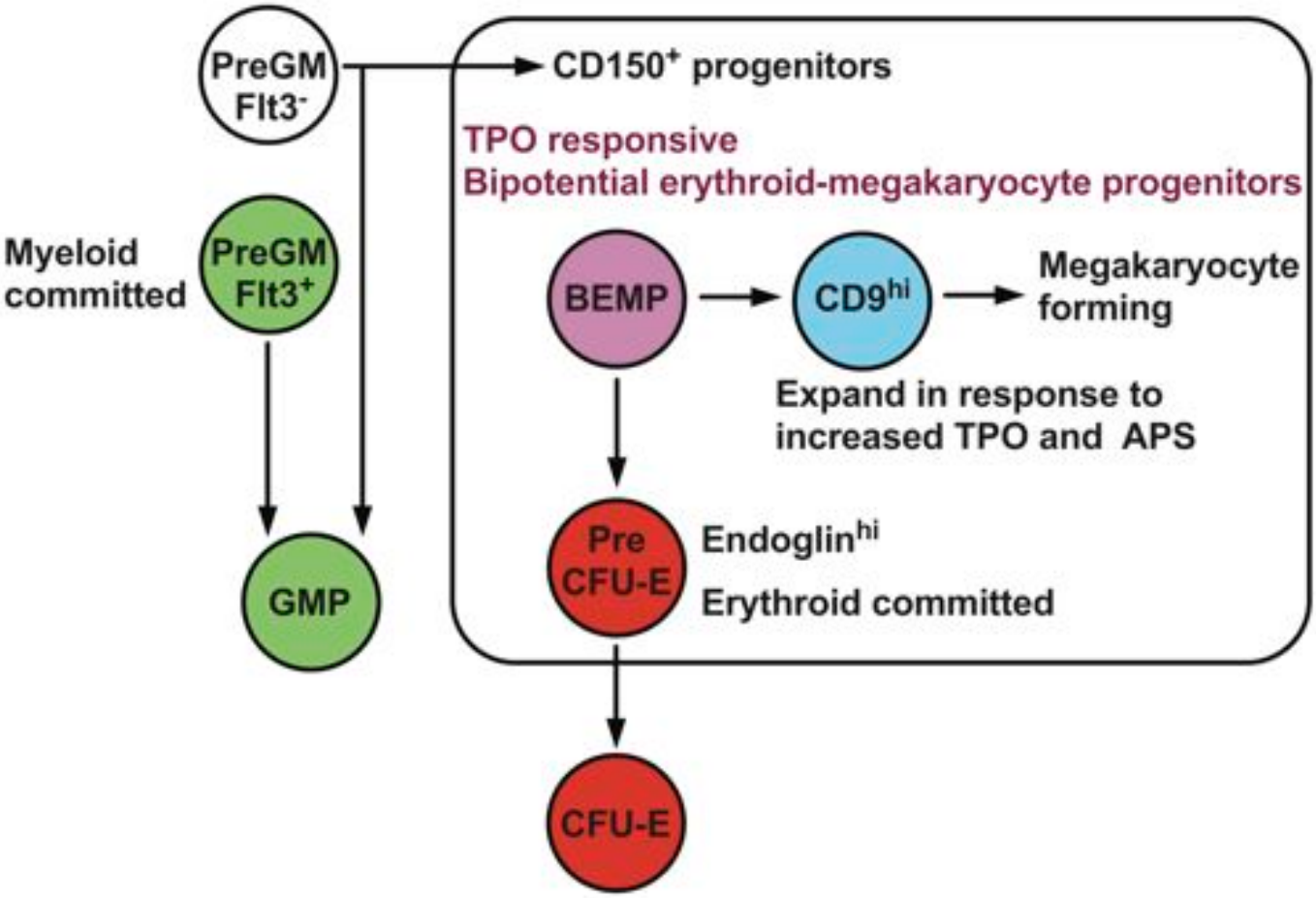
PreGM
Flt3-
CD150+ progenitors
TPO responsive
Bipotential erythroid-megakaryocyte progenitors
Myeloid
committed
PreGM
Flt3+
BEMP
CD9hi
Megakaryocyte
forming
Expand in response to
increased TPO and APS
GMP
Pre
CFU-E
Endoglinhi
Erythroid committed
CFU-E

Table 1. Colony-forming potential of fractions of $Lin^{-}cKit^{+}IL7R\alpha^{-}Fc\gamma RII/III^{lo}Endoglin^{lo}$ adult bone marrow

	Colonies per 100 cells plated							
	Blast	**G**	**GM**	**M**	**Eo**	**Meg**	**% of $cKit^{+}$ fraction**	**Meg contribution**
$Sca1^{-}CD48^{+}CD150^{-}$	2±1	14±5	9±2	10±1	0±0	7±1	36±2	21%
$Sca1^{-}CD48^{+}CD150^{+}$	0.2±0.2	0.1±0.1	0.0±0.1	0.3±0.2	0±0	24±1	37±2	68%
$Sca1^{+}$	18±5	1±1	3.5±4	9±4	0±0	3±2	19±1	11%

Table 2. Colony-forming potential of fractions of $Lin^{-}cKit^{+}Sca1^{-}IL7R\alpha^{-}Fc\gamma RII/III^{lo}CD150^{+}$ adult bone marrow

	Clonogenic colonies per 100 cells plated						% of $CD150^{+}$ fraction	Meg contribution
	Blast	**G**	**GM**	**M**	**Eo**	**Meg**		
$CD9^{lo}Endoglin^{lo}$ (BEMP)	0.5±0.5	0.2±2	0.2±0.2	0.2±0.2	0±0	28±9	51±4.9	92%
$CD9^{hi}Endoglin^{lo}$	0.5±0.6	0.1±0.2	0.2±0.4	0.3±0.3	0±0	10±4	13±2.3	8%
$CD9^{lo}Endoglin^{hi}$ (PreCFU-E)	0±0	0±0	0.2±0.3	0±0	0±0	0.5±0.3	36±5.8	0%

Table S1. Immunophenotypic definitions of selected myeloid progenitor cell populations

Subset	Immunophenotype
PreGM (1)	$Lineage^{-}IL7R\alpha^{-}cKit^{+}Sca1^{-}CD150^{-}Endoglin^{-}FcγRII/III^{-}$
PreCFU-E (1)	$Lineage^{-}IL7R\alpha^{-}cKit^{+}Sca1^{-}FcγRII/III^{-}CD41^{-}CD150^{+}Endoglin^{hi}$
CFU-E (1)	$Lineage^{-}IL7R\alpha^{-}cKit^{+}Sca1^{-}CD150^{-}Endoglin^{+}FcγRII/III^{-}$
PreMeg-E (1)	$Lineage^{-}IL7R\alpha^{-}cKit^{+}Sca1^{-}FcγRII/III^{-}CD41^{-}CD150^{+}Endoglin^{-}$
$CD41^{hi}$MkP (1)	$Lineage^{-}cKit^{+}Sca1^{-}FcγRII/III^{-}CD150^{+}CD41^{+}$
$CD9^{hi}$MkP (2)	$Lineage^{-}IL7R\alpha^{-}cKit^{+}CD9^{+}CD41^{+}FcγRII/III^{-}$
$CD41^{-}$MEP (3)	$Lineage^{-}IL7R\alpha^{-}cKit^{+}Sca1^{-}CD150^{+}CD41^{-}$

Table S2. Colony-forming potential of Flt3$^+$ and Flt3$^-$ fractions of PreGM progenitor cells

	Blast	G	GM	M	Eo	Meg
PreGM Flt3$^+$	2±1	11±4	25±7*	23±4*	0±0	0.3±0.3
PreGM Flt3$^-$	2±0.6	20±3	7±2	7±3	0±0	18±3.5*

Mean colony counts ± standard deviations per 100 cells from three replicate experiments using a combined stimulus of SCF, IL-3 and EPO. G, granulocyte; GM, granulocyte-macrophage; M, macrophage; Eo, eosinophil; Meg, megakaryocyte colonies, including colonies of megakaryocytes and erythroid cells. *$P_{adj} < 0.05$ for comparison by unpaired t-test, with Holm modification of Bonferroni correction for multiple testing.

SI Figure Legends

SI Figure 1. Identification of megkaryocyte colony forming potential in $CD150^+$ and $CD150^-$ cells by flow cytometric purification and semi-solid agar colony assays. (A) Fractionation of $Lin^-cKit^+IL7R\alpha^-Fc\gamma RII/III^{lo}Endoglin^{lo}$ bone marrow cells using cKit, Sca1, CD150 and CD48 antigens to identify progenitors with megakaryocyte colony forming potential. Proportional contributions of gated fractions to parental populations are shown as means ± standard deviations from 4 mice. (B-E) Representative images of megakaryocyte containing colonies from the $Lin^-cKit^+Sca1^-IL7R\alpha^-Fc\gamma RII/III^{lo}Endoglin^{lo}CD150^+CD48^+$ bone marrow fraction grown in semi-solid agar after fixation and staining with acetylcholinesterase, luxol fast blue and hematoxylin. Images shown at 40X magnification with inset images 1000X magnification. (B) Classical mature megakaryocyte colony with large cells containing acetylcholine esterase positive cytoplasm. (C) megakaryocyte colony with cellular morphology demonstrating scant acetylcholine esterase positive cytoplasm. (D) megakaryocyte colony with atypical acetylcholine esterase positive cytoplasmic morphology. (E) bipotential erythroid/megakaryocyte colony showing acetylcholine esterase positive megakaryocytes interspersed amongst erythroblasts. Images acquired using a Nikon Eclipse E600 microscope, using 40x/1.3 NA objective or 100x/1.3 NA oil objective with AxioCam Hrc and AxioVision 3.1 image acquisition software.

SI Figure 2. Fractionation of Lin$^-$cKit$^+$Sca1$^-$IL7Rα$^-$FcγRII/III^{lo}CD150$^+$ bone marrow with CD9 and Endoglin. Immunophenotypic comparison of CD9^{lo}Endoglin^{lo}, CD9^{hi}Endoglin^{lo} and CD9^{lo}Endoglin^{hi} fractions of Lin$^-$cKit$^+$Sca1$^-$IL7Rα$^-$ FcγRII/III^{lo}CD150$^+$ bone marrow with previously defined CD41^{hi}MkP and CD41$^-$MEP populations (Table S1) using multi-parameter flow cytometry for simultaneous analysis of antigen expression.

SI Figure 3. *In vitro* responses of Lin$^-$cKit$^+$Sca1$^-$IL7Rα$^-$FcγRII/III^{lo}CD150$^+$ progenitor cells to cytokine stimulation. Differentiation of CD9^{hi}Endoglin^{lo} and CD9^{lo}Endoglin^{hi} fractions of Lin$^-$cKit$^+$Sca1$^-$IL7Rα$^-$FcγRII/III^{lo}CD150$^+$ bone marrow cells in liquid culture after 4 days with the cytokine combinations indicated. *P_{adj}<0.05 when compared to SCF, IL3 and EPO, **P_{adj} < 0.05 when compared to SCF and EPO, with Holm modification of Bonferroni correction for multiple testing.

SI Figure 4. Characterization of lineage$^-$cKit$^+$Sca1$^-$CD150$^-$Endoglin$^-$FcγRII/III$^-$ PreGM progenitors. (A) May-Grunwald-Giemsa stained cytocentrifuge preparations of differentiated cells derived from PreGM progenitors grown in liquid culture with cytokine combinations as indicated (SCF, 20ng/mL; IL-3, 10ng/mL; EPO, 2IU/mL; TPO, 200ng/mL). Images were acquired under oil immersion using Nikon Eclipse E600 microscope, 100x/1.3 NA Oil objective with AxioCam Hrc and AxioVision 3.1 image acquisition software. (B) Immunophenotype of cells derived from PreGM progenitors in liquid culture with cytokine combinations as shown after 4 days. CD9^{hi}CD150$^+$

megakaryocytes (blue), Endoglin^{hi}CD150^{-}CD9^{lo} erythroid progenitors (red) and FcγRII/III^{hi} granulocyte progenitors (green). *$P < 0.05$ when compared to PreGM progenitors culture in SCF, IL3 and EPO. (C) Proliferation of 1000 PreGM progenitors cultured with cytokine combinations as shown after 4 days in liquid culture. *P_{adj}<0.02 when comparing SCF and TPO to SCF, IL3 and EPO, **P_{adj}<0.006 when comparing SCF and TPO to SCF and TPO, with Holm modification of Bonferroni correction for multiple testing. (D) Percentage of Endoglin^{hi} erythroid progenitors, CD9^{hi}CD150^{+} megakaryocytes, or FcγRII/III^{+} granulocytes derived from PreGM progenitors in liquid culture after 4 days, with combinations of cytokines as shown. (E) Proportion of CD9^{hi}CD150^{+} megakaryocytes differentiated from PreGM progenitors after 4 days in liquid culture with cytokine combinations as shown. *P_{adj}<0.03 when comparing SCF and TPO to SCF, IL3 and EPO, with Holm modification of Bonferroni correction for multiple testing. (F) Generation of GMP, CMP and MEP (left panels) and PreCFU-E and CFU-E (middle panels) and CD150^{+} progenitors (right panels) from 2000 GFP-marked (4) Flt3^{+} PreGM cells (upper panels) and Flt3^{-} PreGM cells (lower panels) following transplantation into sublethally irradiated recipients. Profiles show analysis of Lin^{-}cKit^{+} bone marrow cells at 7 days after transplantation with GFP-marked donor (4) contribution to the indicated progenitor populations shown in red, and recipient populations shown as a contour plots in gray. Representative analysis of three independent donors is shown.

SI Materials and Methods

Mice

For analysis of erythroid and platelet reconstitution by sorted cell populations, C57BL/6 mice were exposed to a single sublethal dose of 475cGy of γ-irradiation, and injected via the tail vein with 1000 GFP^{pos} cells (4). Blood from the tail was analyzed on days 4, 7 and 12 following transplantation. Analysis of lineage negative bone marrow from 3-4 pooled recipients was performed at 4 and/or 7 days after injection of 1000 or 2000 GFP^{pos} cells per sublethally irradiated recipient.

Hematology and histology

Flow cytometric analysis of erythrocytes and platelets was performed after blood was suspended in buffered saline glucose citrate buffer (BSGC: 116 mM NaCl, 13.6 mM trisodium citrate, 8.6 mM Na_2HPO_4, 1.6 mM KH_2PO_4, 0.9 mM Na_2EDTA, 11.1 mM glucose). Single cell suspensions from bone marrow were prepared in balanced salt solution (BSS-CS: 0.15 NaCl, 4 mM KCl, 2 mM $CaCl_2$, 1 mM $MgSO_4$, 1 mM KH_2PO_4, 0.8 mM K_2HPO_4 and 15 mM HEPES supplemented with 2% vol/vol bovine calf serum). Clonal analysis of bone marrow cells in semi-solid agar cultures were performed in 1 mL volumes of 0.3% agar in Iscove modified Dulbecco medium containing 20% newborn calf serum using a combined stimulus of stem cell factor (SCF, 100ng/mL), interleukin 3 (IL-3, 10ng/mL), and erythropoietin (EPO, 4IU/mL), incubated for 7 days in a fully humidified atmosphere of 5% CO_2 in air. Cultures were then fixed, dried onto glass slides, and stained for acetylcholinesterase, then with luxol fast blue and hematoxylin, and the number and type of colonies were determined by microscopic examination.

Liquid cultures were performed in StemPro-34 Serum-free Medium with Nutrient Supplement (Invitrogen) with cytokines added as indicated (SCF, 20ng/mL; IL-3, 10ng/mL; EPO, 2IU/mL; TPO, 200ng/mL).

Flow Cytometry

Antigen staining was performed using rat-anti-mouse biotinylated or fluorochrome-conjugated antibodies specific for Ter119 (Ly-76), Gr1 (Ly6G and Ly6C), Mac1 (CD11b), B220 (CD45R), CD4, CD8, CD41, CD16/32, Sca1(Ly6A/E), CD34, CD135 (BD Pharmingen), cKit (CD117), CD150 (Biolegend), IL7Rα, CD48, CD105, and CD9, (eBioscience). Secondary staining used goat-anti-rat Alexa Fluor 700 (Invitrogen) or streptavidin Phycoerythrin Texas Red (BD Pharmingen). Cells were analysed using an LSRII (Becton Dickinson) or sorted using a FACS Aria II (Becton Dickinson) flow cytometers. Lineage depletion of Ter119 (Ly-76), Gr1 (Ly6G and Ly6C), Mac1 (CD11b), B220 (CD45R), CD4, CD8, IL7Rα was performed with rat-anti-mouse or biotinylated lineage antibodies, and depleted using goat anti-rat or anti-biotin MACS MicroBeads on MACS LS columns according to manufacturer instructions (Miltenyi Biotec), prior to sorting of stained bone marrow cells.

Statistical analysis

Student unpaired 2-tailed *t* tests were used with Holm modification of Bonferroni correction for multiple testing (5). Comparison of PU.1 mean fluorescence intensity for progenitor populations was performed with repeated measures ANOVA, and Tukey's multiple comparison of means, and correlation analysis was performed with Pearson correlation using GraphPad Prism version 5.0a for Mac Os X (GraphPad Software, La Jolla California USA, www.graphpad.com).

References

1. Pronk CJ*, et al.* (2007) Elucidation of the phenotypic, functional, and molecular topography of a myeloerythroid progenitor cell hierarchy. *Cell Stem Cell* 1(4):428-442.
2. Nakorn TN, Miyamoto T, & Weissman IL (2003) Characterization of mouse clonogenic megakaryocyte progenitors. *Proc Natl Acad Sci U S A* 100(1):205-210.
3. Rieger MA, Smejkal BM, & Schroeder T (2009) Improved prospective identification of megakaryocyte-erythrocyte progenitor cells. *Br J Haematol* 144(3):448-451.
4. Schaefer BC, Schaefer ML, Kappler JW, Marrack P, & Kedl RM (2001) Observation of antigen-dependent CD8+ T-cell/ dendritic cell interactions in vivo. *Cell Immunol* 214(2):110-122.
5. Holm S (1979) A simple sequentially rejective multiple test procedure. *Scandinavian Journal of Statistics*:65-70.

Figure S1

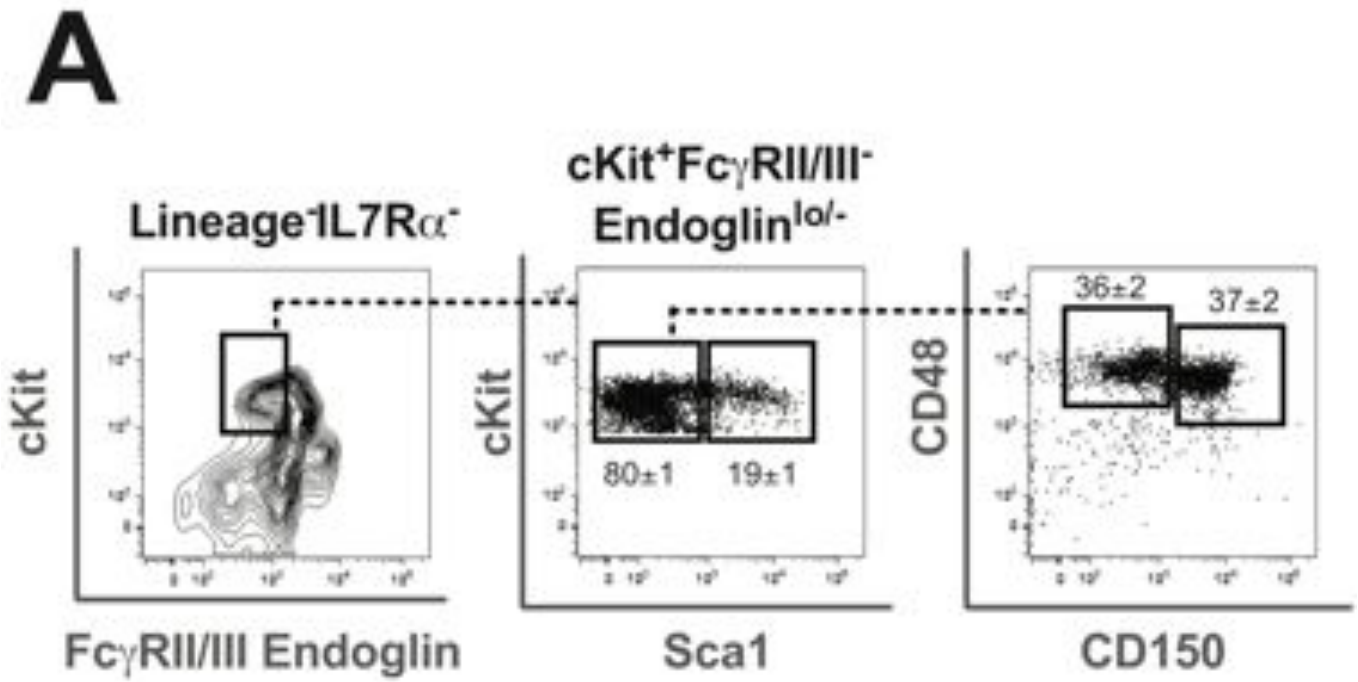
A
Lineage⁻IL7Rα⁻
cKit⁺FcγRII/III⁻
Endoglin^lo/-
cKit
FcγRII/III Endoglin
cKit
Sca1
80±1
19±1
CD48
CD150
36±2
37±2

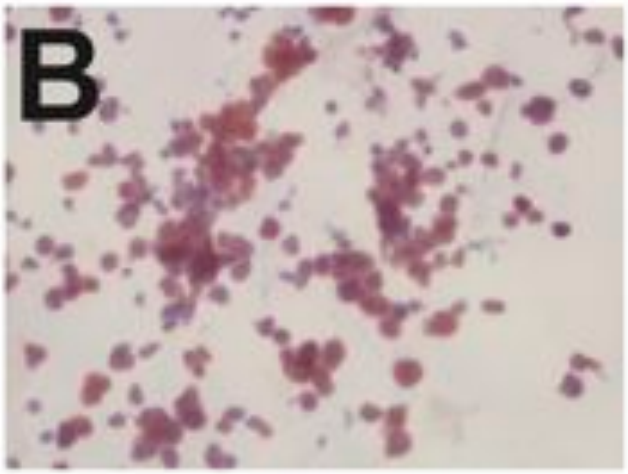
B

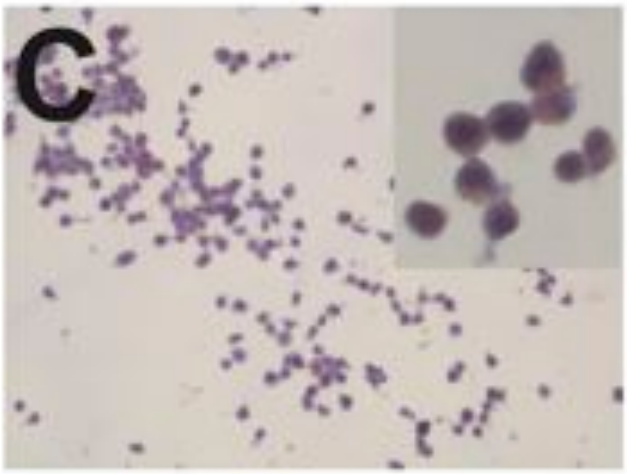
C

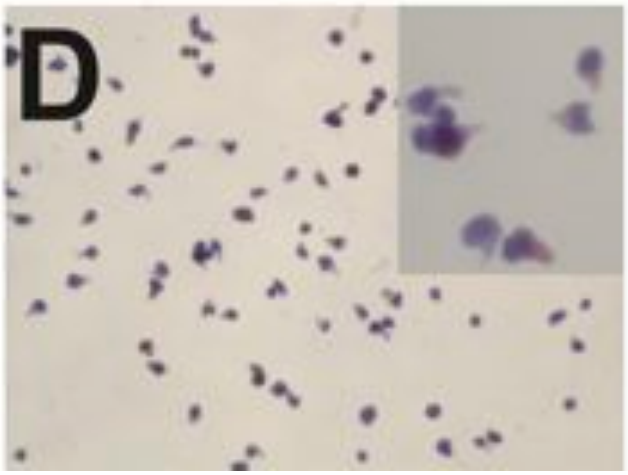
D

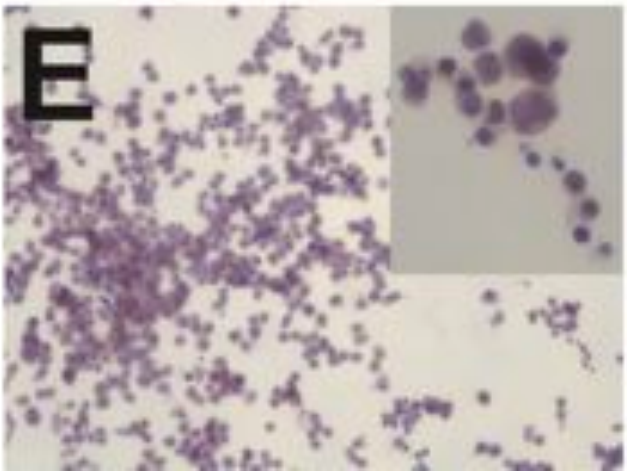
E

Figure S2

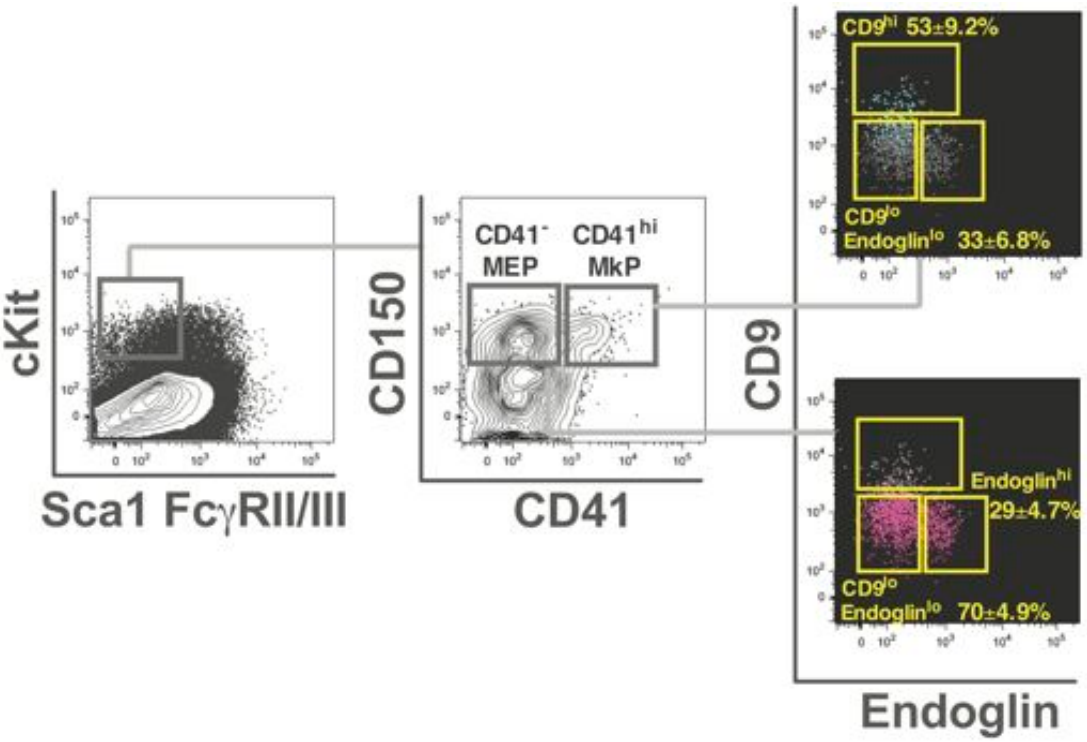
cKit
Sca1 FcγRII/III
CD150
CD41
CD41- MEP
CD41hi MkP
CD9
CD9hi 53±9.2%
CD9lo Endoglinlo 33±6.8%
Endoglinhi 29±4.7%
CD9lo Endoglinlo 70±4.9%
Endoglin

Figure S3

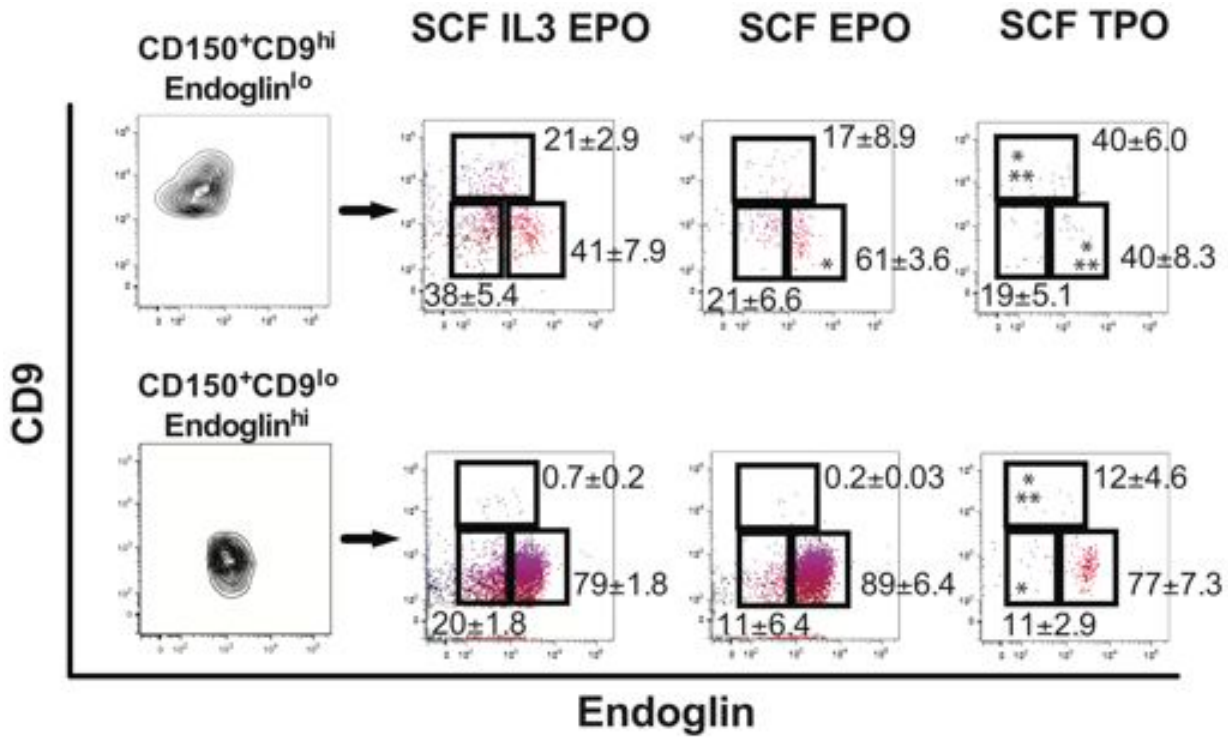
SCF IL3 EPO
SCF EPO
SCF TPO
CD150+CD9hi
Endoglinlo
CD150+CD9lo
Endoglinhi
21±2.9
41±7.9
38±5.4
17±8.9
61±3.6
21±6.6
40±6.0
40±8.3
19±5.1
0.7±0.2
79±1.8
20±1.8
0.2±0.03
89±6.4
11±6.4
12±4.6
77±7.3
11±2.9
CD9
Endoglin

Figure S4

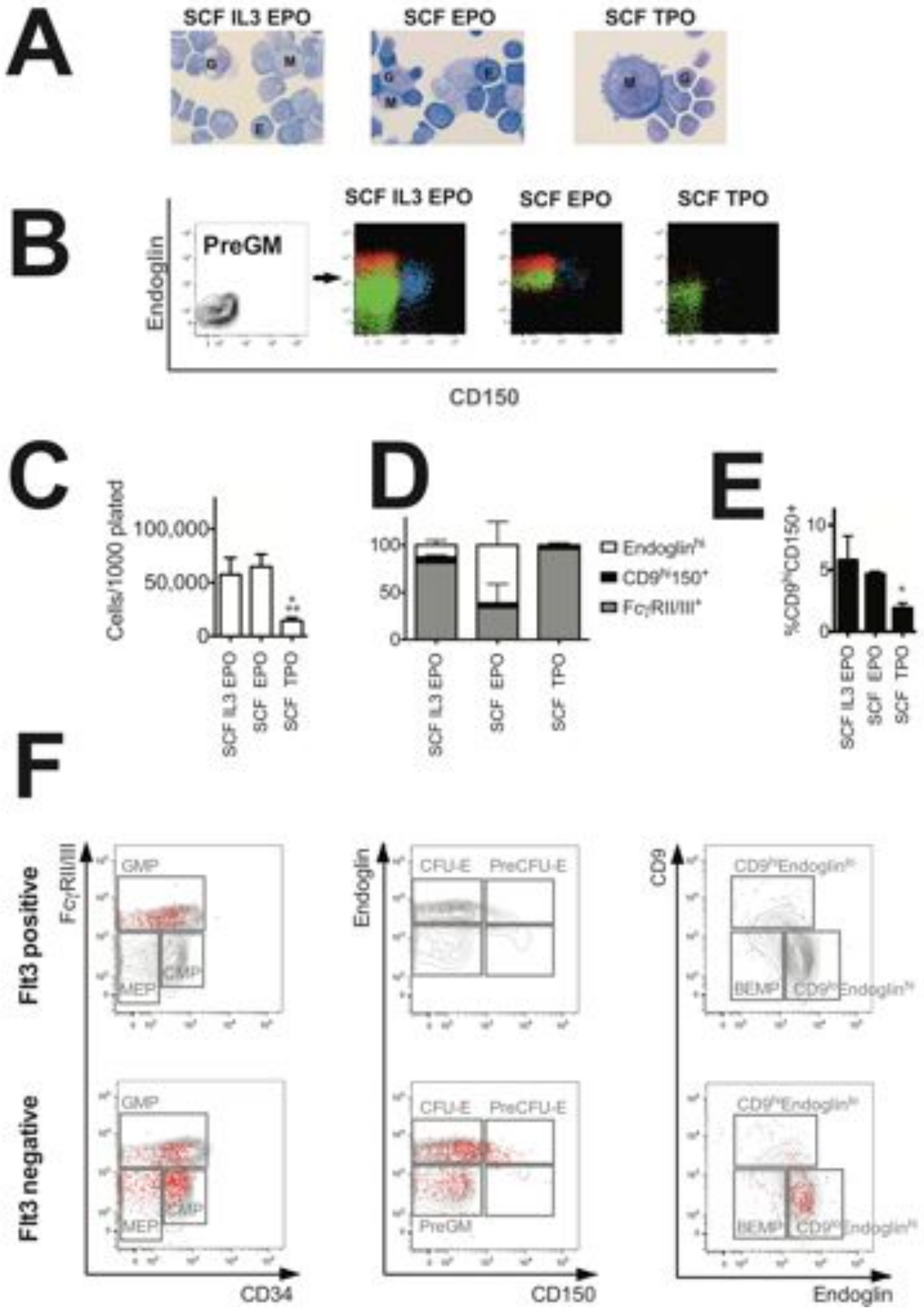
A
SCF IL3 EPO
SCF EPO
SCF TPO
B
PreGM
Endoglin
CD150
SCF IL3 EPO
SCF EPO
SCF TPO
C
Cells/1000 plated
100,000
50,000
0
SCF IL3 EPO
SCF EPO
SCF TPO
D
100
50
0
Endoglin^hi
CD9^hi150+
FcγRII/III+
SCF IL3 EPO
SCF EPO
SCF TPO
E
%CD9^hiCD150+
10
5
0
SCF IL3 EPO
SCF EPO
SCF TPO
F
Flt3 positive
Flt3 negative
FcγRII/III
GMP
MEP
CMP
CD34
Endoglin
CFU-E
PreCFU-E
PreGM
CD150
CD9
CD9^hiEndoglin^hi
BEMP
CD9^hiEndoglin^lo
Endoglin